

Simulation of Cup-Burner Flames in Microgravity

Viswanath R. Katta*
Innovative Scientific Solutions Inc.
2766 Indian Ripple Road, Dayton, OH 45440

Fumiaki Takahashi
National Center for Microgravity Research on Fluids and Combustion
NASA Glenn Research Center
21000 Brookpark Road, Cleveland, OH 44135

and

Gregory T. Linteris
Fire Research Division, National Institute of Standards and Technology
Gaithersburg, MD 20899

Abstract

The extinction process of cup-burner flames under normal-gravity conditions were previously studied. As the low-speed diffusion flames behave differently in microgravity compared to those on earth, it is important to understand the structure of cup-burner flame and its extinction characteristics under 0g conditions. A numerical study was performed in the present paper using a time-dependent, axisymmetric model and by incorporating detailed chemical kinetics of CH₄ and O₂. Calculations were performed for the cup-burner flame under different gravitational forces. It was observed that the cup-burner flame ceases to flicker under gravitational forces less than 0.5g. As the buoyancy force was reduced, the flame diameter increased, the tip of the flame opened, and the flame at the base became vertical. Through numerical experiments it was found that radiative heat loss was predominantly responsible for the extinction of flame in the tip region under 0g conditions. In contrast, 1g flames were not affected much by the radiative heat loss.

Introduction

A fire, whether within a spacecraft or in an occupied space on extraterrestrial bases can lead to mission termination or loss of life. The advent of longer duration missions to the moon, Mars, or aboard the space stations increases the likelihood of fire mishaps. Therefore, development of efficient fire safety systems and procedures for the space-oriented living represents a mission-critical task. This requires an understanding of the inhibition mechanisms of fire-suppressing and inert agents in microgravity flames.

Experimental or numerical studies for the investigation of the inhibitory effects of halogenated hydrocarbons on flames have been performed in either premixed^{1,2} or diffusion systems.^{3,4} Premixed flames are selected mainly because the overall reaction rate, heat release, and heat and mass transport can be described with a fundamental parameter—the laminar burning velocity; on the other hand, most common fires are of the diffusion type and often become dynamic in nature with large vortical structures entraining additional surrounding air.

The predominant experimental techniques for studying fire suppression in diffusion flames are the cup-burner and opposing-jet configurations. In both these experiments, agents are quasi-statically added to either the fuel or air stream. The opposed-jet configuration offers very simple flames that can be modeled using one-dimensional analysis and, hence, is often used for the development of chemical kinetics models for different agents. From a fire safety point of view, however, the most hazardous situation is a low-strain-rate diffusion flame such as the one established over a cup burner where flames are more stable and larger concentrations of agent are required to achieve extinction. Studies on cup-burner flames are also important since the amount of agent required for extinguishing these flames is believed to scale to the requirements in common fires.

Under normal gravitational conditions, a laminar jet diffusion flame formed over a cup burner with negligibly small fuel flow rate and a low-speed annular air flow develops large-scale, low-frequency (1-40 Hz), organized buoyancy-induced vortices on the air side of the flame.

* Corresponding author: vrkatta@erinet.com

Both experimental^{5,6} and numerical⁷ studies have been performed on these dynamic flames to identify the differences in agent requirements established using opposing-jet and cup-burner flames. On the other hand, several studies^{8,9} have pointed out that the low-speed, coaxial, jet diffusion flames similar to those associated with cup burners behave differently under microgravity. As a result, the agent requirements for extinguishing the cup-burner flames could be different from those established based on ground-based studies.

This paper describes an investigation performed using a two-dimensional numerical model with detailed kinetics, developed for the simulation of dynamic jet diffusion flames, for establishing extinction criterion of cup-burner flames in microgravity. Numerical experiments are performed to understand the dramatic structural differences observed between the cup-burner flames operating under normal- and micro-gravity conditions.

Description of Cup Burner

The cup burner, described previously,^{5,6,7} was used for the present investigations of gravity effects on flame-extinction process. It consists of a cylindrical glass cup (28-mm diameter) positioned inside a glass chimney (53.3-cm tall, 9.5-cm diameter). The air velocity in the absence of agents is (10.7 ± 0.21) cm/s, and the fuel jet velocity is (0.921 ± 0.018) cm/s. The fuel gas is methane, the agent is CO₂ (Airgas), and the air is house compressed air (filtered and dried), which is additionally cleaned by passing it through a 0.01 μ m filter, a carbon filter, and a desiccant bed to remove small aerosols, organic vapors, and water vapor.

Computational Model

A time-dependent, axisymmetric mathematical model known as UNICORN (Unsteady Ignition and Combustion using ReactionNs)¹⁰ is used for the simulation of unsteady jet diffusion flames associated with the cup burner. It solves for axial and radial (*z* and *r*) momentum equations, continuity, and enthalpy- and species-conservation equations on a staggered-grid system. The body-force term due to the gravitational field is included in the axial-momentum equation to simulate upward-oriented flames. A clustered mesh system is employed to trace the gradients in flow variables near the flame surface. A detailed chemical-kinetics model GRI-V1.2 (developed by the Gas Research Institute)¹¹ is incorporated in UNICORN for the investigation of CO₂ effects on methane combustion. This mechanism for methane flames is comprehensive, with 31 species and 346 elementary reactions. Temperature and species dependent thermophysical properties such as enthalpy, viscosity, thermal conductivity, and binary molecular diffusion were used. A simple radiation model based on optically thin-media assumption was incorporated into the energy

equation. Only radiation from CH₄, CO, CO₂, and H₂O was considered in the present study.¹²

The finite-difference forms of the momentum equations are obtained using an implicit QUICKEST scheme,¹³ and those of the species and energy equations are obtained using a hybrid scheme of upwind and central differencing. At every time-step, the pressure field is accurately calculated by solving all the pressure Poisson equations simultaneously and utilizing the LU (Lower and Upper diagonal) matrix-decomposition technique.

Calculations for the cup-burner flames are made on a physical domain of 200 x 47.5 mm utilizing a 251 x 101 non-uniform grid system that yielded 0.2-mm grid spacing in both the *z* and *r* directions in the flame zone. Flat velocity profiles are imposed at the fuel and air inflow boundaries, while an extrapolation procedure with weighted zero- and first-order terms is used to estimate the flow variables at the outflow boundary. For the accurate simulation of flow structure at the base of the flame, which is very important in the flame-extinction studies, the fuel cup wall was treated as a 1-mm long and 1-mm thick tube in the calculations. The temperature of this tube was set at 600 K, which is very close to that measured in the experiment.

Results and Discussion

The fuel and air velocities of 0.921 and 10.7 cm/s, respectively, used in the present investigation represent a weakly strained flame. Under the influence of gravitational force, the low annular air velocity promotes the buoyancy-induced instabilities outside the flame surface and makes the flame to flicker at a low frequency. The computed instantaneous flowfield of the pure CH₄/air flame is shown in Fig. 1(a). The CO₂-iso-molar-concentration and temperature distributions are shown on the left and right halves, respectively. The velocity and iso contours of H₂ are superimposed on the temperature and CO₂ distributions, respectively. Except in the base region ($0.1 < z < 4$ mm), the peak temperature of the flame is constant everywhere at 1880 K. The flame height at the instant shown in Fig. 1(a) is ~ 64 mm.

To investigate the effects of gravitational force on cup-burner flames, calculations were repeated for different gravitational-force conditions. Results for 0g are shown in Fig. 1(b). The salient features noted from a comparison of flame structures obtained under different gravitational-force conditions are: 1) flames became steady state when gravitational force was $< 0.5g$, 2) flame height decreased and diameter increased with reduction in gravitational force, 3) peak velocity at a height of 80 mm above the burner decreased from ~ 2.2 m/s to ~ 0.2 m/s when gravity was reduced from 1g to 0g, 4) peak temperature decreased slightly but, more importantly, temperature of the flame tip decreased dramatically with reduction in gravitational force, and finally, 5) the severely concaved flame near the

burner rim became parallel to the fuel jet when gravitational force was reduced from 1g to 0g.

Flame structure shown in Fig. 1(b) for 0g case represents an open-tipped flame. In fact, decreasing gravitational force on a cup burner flame generated dramatic changes to its structure. At 1g, the flame was severely oscillating with pockets of fuel being pinched off from the jet and burning independently [Fig. 1(a)]. At 0.5g, a closed-tip, steady-state flame was generated. Finally, for gravitational force $< 0.2g$, flame became completely open-tipped with burning taking place only in the shoulder region. Formation of closed contours of 0.02 X_{H_2} in these flames in the base region suggests that H_2 is no longer produced at the flame tip.

As described earlier, radiation from CH_4 , CO , CO_2 , and H_2O was included in the present calculations. A simple radiation model based on optically thin-media assumption was used. As suggested by Easton et al.,¹⁴ radiative heat losses could become a dominating heat-transfer mechanism when the generation of heat is decreased due to lack of reactant convection. To verify this, radial distributions of heat release rate and radiative heat loss at 20 mm above the burner are plotted in Fig. 2 for different g cases. This height represents the farthest location from the burner rim where flame exists in all g cases. Fig. 2 shows that heat release rate decreases significantly with reduction in gravitational force. For 0g case the maximum heat release rate is only $1/3^{rd}$ of that obtained for 1g case. Since, flame temperatures are nearly the same at this location for all the cases, reduction in heat release rate can be attributed to the reduction in reactant fluxes into the flame zone. The drastic decrease in convective flow in lower g cases is limiting the reactant fluxes in to the flame zone. On the other hand, radiative heat losses are more or less the same in all g cases. The dominance of radiative heat loss in low-g cases is causing the flame to extinguish in the downstream locations.

To further verify that the radiative heat losses are indeed causing the flame to extinguish at the tip, numerical experiments have been performed on 0g flame. Three different calculations were made for this flame: 1) by ignoring radiation in the energy equation, 2) by ignoring finite-rate chemistry, and 3) by ignoring both radiative heat loss and finite-rate chemistry. The flow conditions and numerical details used for these calculations were the same as those used for the flame (0g case) shown Fig. 1(b). All three calculations converged to steady-state flames even though unsteady simulations were performed.

The 0g flame computed with no radiation is shown in Fig. 3 with a plotting scheme same as that used for Fig. 1(b). Surprisingly, in the absence of radiation, flame became a closed-tip one with burning taking place along the flame surface from base to the tip at the centerline. The peak flame temperature has increased by ~ 150 K but, more interestingly, temperature all along the flame surface became nearly the same. The closed contours of

H_2 in Fig. 1(b) disappeared in Fig. 3 indicating that combustion is taking place all the way up to the flame tip when the radiation is turned off in the calculations. Due to this increased burning (and volumetric expansion) the local velocity has increased by $\sim 35\%$ at $z = 80$ mm compared to that in 0g flame shown in Fig. 1(b).

Flames resulting from the calculations made by using infinitely-fast-chemical-kinetics model are shown in Fig. 4. The iso-temperature color plots of the flames without and with radiation are shown in the left and right halves, respectively. The structures of these flames became similar to their counter parts computed with finite-rate chemistry. The infinitely fast chemistry flame computed with radiation is similar to the one shown in Fig. 1(b) and the flame computed without the radiative heat loss is similar to that shown in Fig. 3 (right side). These comparisons further suggest that finite-rate chemistry of methane-air combustion did not cause the tip quenching seen in 0g and low-g flames. Calculations were also performed for 0g flame by using unity-Lewis number assumption. The resulted flame with radiative heat losses had a flame structure that is similar to that shown in Fig. 1(b). This suggests that neither curvature nor preferential diffusion are responsible for the tip opening of the 0g flame. Analysis of all the results obtained from different numerical experiments suggests that radiative heat losses are predominantly responsible for the quenching phenomenon seen in microgravity cup-burner flames.

To understand how radiation is affecting only the low-g flames, calculations for the 1g flame were also repeated by turning off the radiative heat losses in the energy equation. The flame resulted from this simulation is shown in Fig. 5. Even though, there exists some minor differences in the flame temperatures, over all, 1g flames obtained with [Fig. 1(a)] and without (Fig. 5) the radiative heat losses are similar in structure. Tips of both the flames are closed with burning taking place all along the flame surface. Both the flames are flickering and resulting in pinching off of fuel pockets at the tip. However, the flickering frequency is increased to 12.5 Hz. when the radiative heat loss was ignored in the calculations. An additional vortex is forming in Fig. 5 in addition to those formed in Fig. 1(a). This should be expected as the buoyancy forces are slightly increased with an increase in flame temperature in Fig. 5.

The temperature and axial velocity along the flame surface obtained with and without radiation are plotted for the 0g flame in Fig. 6(a) and for the 1g flame in Fig. 6(b). In all the calculations temperature and axial velocity have increased initially in the flame base region. However, in case of 0g, flame temperature remained more or less constant around 2000 K in the downstream locations when radiation was ignored and decreased linearly from 1850 K when radiation was included in the calculations. It was found from earlier calculations⁷ that stoichiometric methane diffusion flames quench when temperature is

dropped below 1550 K. Based on this it can be assumed that the 0g flame (computed with radiative heat loss) was quenched at locations $z > 35$ mm. Absence of combustion in these locations resulted in a constant axial velocity of ~ 0.22 m/s, where as, it is increasing monotonically when radiation was turned off.

In the case of 1g flame, calculations made with and without the radiative heat losses yielded flame temperatures that are nearly constant [Fig. 6(b)]. In both calculations axial velocities are increasing with z due to buoyancy and thermal expansion of gases. The higher axial velocities in the case of 1g flame (~ 1 m/s compared to 0.22 m/s in 0g case) are resulting in higher reactant fluxes into the flame zone and, in turn, increasing the heat release rates high enough to overcome the heat losses due to radiation. As a result, radiation did not have much effect on the 1g flame.

The fuel and oxidizer fluxes in the vicinity of the flame surface are compared in Fig. 7 for the normal-gravity (left) and microgravity (right) conditions. The locations of the flame are identified via plotting near-peak-temperature contours. It is evident from this plot that the amount of fuel and oxygen penetrating into the combustion products has significantly reduced under microgravity conditions. In the presence of radiative heat loss, this mixing is not sufficient to keep the flame temperature above the quenching limit, hence, extinction occurred at locations downstream of $z = 20$ mm.

Conclusions

Pure-methane-air diffusion flames formed over a cup burner under normal-gravity and microgravity conditions were investigated using a time-dependent, axisymmetric CFD model that incorporated a 31-species, 346-reactions chemical-kinetics mechanism (GRI-V1.2). Under normal-gravity conditions, due to small fuel flow rate and a low-speed annular air flow, the laminar cup-burner flame established large-scale, low-frequency (~ 10 Hz), organized vortices on the air side. Calculations were performed for this flame under different gravitational forces. It was observed that the cup-burner flame ceases to flicker for gravitational forces less than 0.5g. As the buoyancy forces were reduced, the flame diameter increased, the tip of the flame extinguished (opened), and the flame at the base became vertical. Through numerical experiments it was found that radiative heat loss was predominantly responsible for the extinction of flame tip under 0g conditions. On the other hand, ignoring radiation in 1g-flame calculation did not have much impact on the flame structure.

Acknowledgements

This work was supported by the Office of Biological and Physical Research, NASA, Washington, D. C. The first author would like to thank Dr. Mel Roquemore of

Wright Laboratory for the stimulating discussions on buoyant flames.

References

1. Linteris, G. T., and Truett, L., *Combust. Flame*, Vol. 105, 1996, p. 15.
2. Linteris, G. T., Burgess, D. R., Jr., Babushok, V., Zachariah, M., Tsang, W., and Westmoreland, P., *Combust. Flame*, Vol. 113, 1998, p. 164.
3. Milne, T. A., Green, C. L., and Benson, D. K., *Combust. Flame*, Vol. 15, 1970, p. 255.
4. Seshadri, K., and Ilincic, N., *Combust. Flame*, Vol. 101, 1995, p. 271.
5. Hirst, B. and Booth, K., *Fire Technol.* 13:296 (1977).
6. Linteris, G.T. and Gmurczyk, G.W., in *Fire Suppression System Performance of Alternative Agents in Aircraft Engine and Dry Bay Laboratory Simulations* (R.G. Gann, Ed.), National Institute of Standards and Technology, Gaithersburg, MD, 1995.
7. Katta, V. R., Takahasi, F., and Linteris, G. T., *Proceedings of the 7th International Symposium on Fire Safety Science*, Worcester, MA, 16-21 June 2002.
8. Hegde, U., Zhou, L., and Bahadori, Y. M., *Combustion Science and Technology*, Vol. 102, 1994, pp. 95-113.
9. Katta, V. R., Goss, L. P., and Roquemore, W. M., *AIAA Journal*, Vol. 32, No. 1, 1994, p. 84.
10. Roquemore W. M., and Katta, V. R., *Journal of Visualization*, Vol. 2, Nos. 3/4, 2000, pp.257-272.
11. Frenklach, M., Wang, H., Goldenberg, M., Smith, G. P., Golden, D. M., Bowman, C. T., Hanson, R. K., Gardiner, W. C., V. Lissianski, V., Technical Report No. GRI-95/0058, Gas Research Institute, Chicago, IL, November 1, 1995.
12. Annon., *Computational Submodels*, International Workshop on Measurement and Computation of Turbulent Nonpremixed Flames., <http://www.ca.sandia.gov/tdf/Workshop/Submodels.html>, 2001.
13. Katta, V. R., Goss, L. P., and Roquemore, W. M., *AIAA Journal*, Vol. 32, No. 1, 1994, p. 84.
14. Easton, J., Tien, J., and Dietrich, D., *First Joint Meeting of the U. S. Sections of the Combustion Institute*, Washington, D.C., March 14-17, 1999, pp. 665-668.

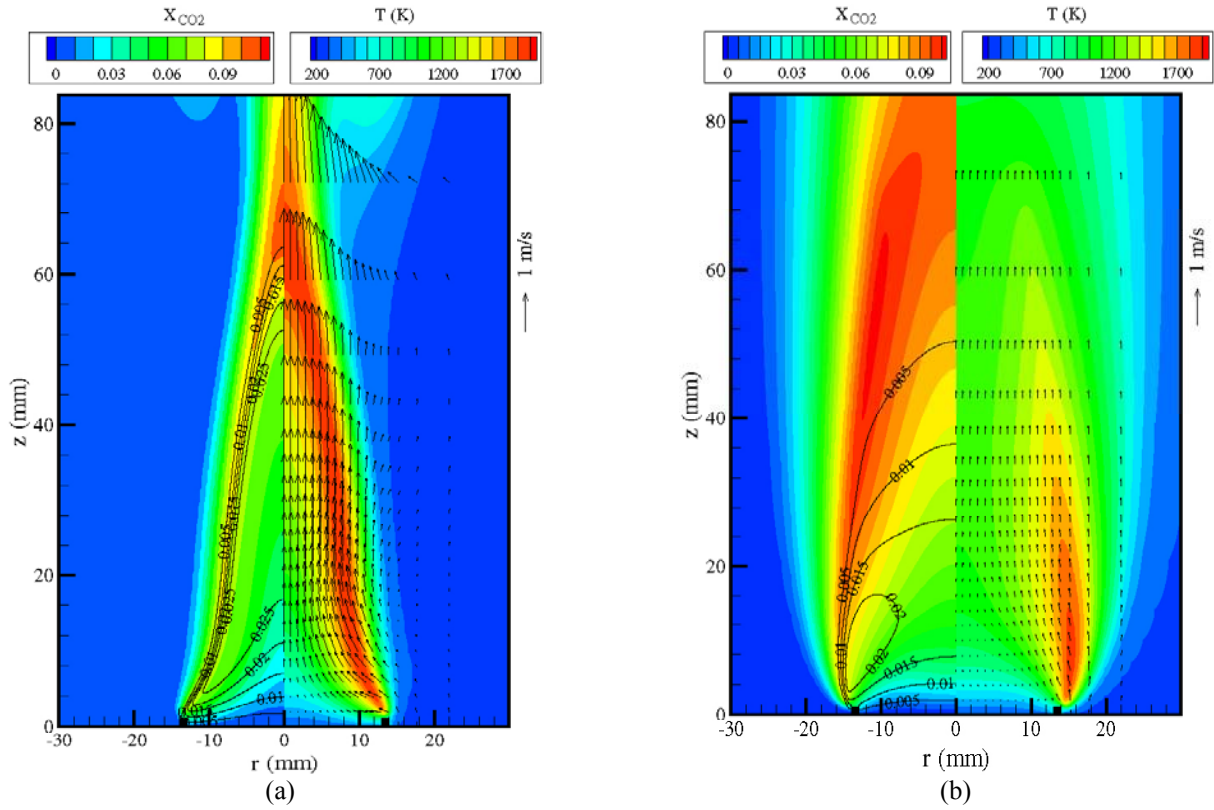


Fig. 1. Structures of cup-burner flame under (a) normal-gravity and (b) microgravity conditions. Temperature and velocity fields are shown on right half and CO_2 and H_2 concentrations are shown on left half.

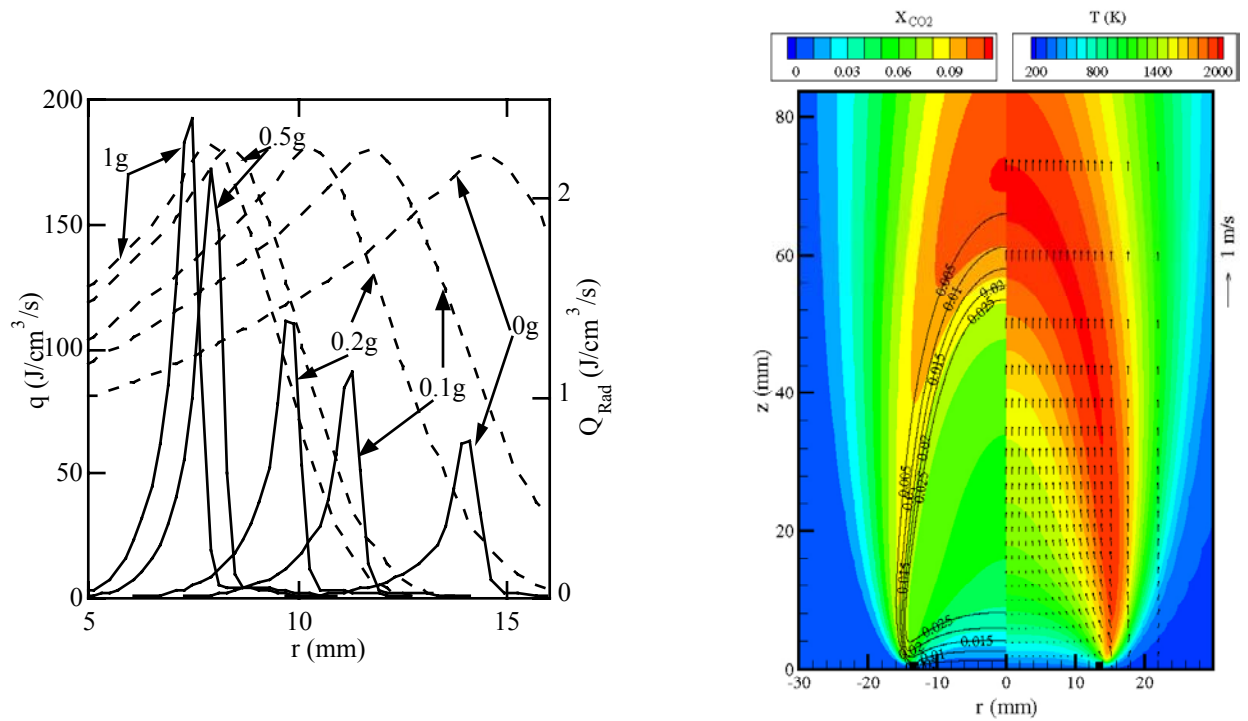


Fig. 2. Distributions of heat release rate q (solid lines) and radiative heat loss Q_{rad} (broken lines) at 20 mm above the burner under different gravitational conditions.

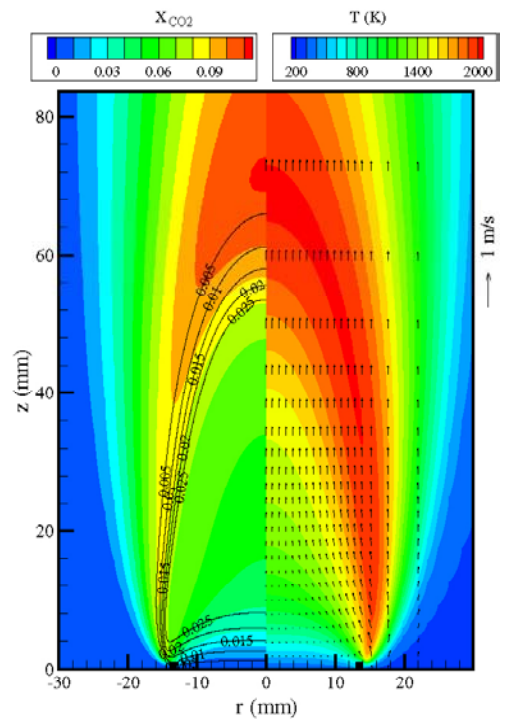


Fig. 3. Cup-burner flame under $0g$ conditions calculated by ignoring radiative heat losses.

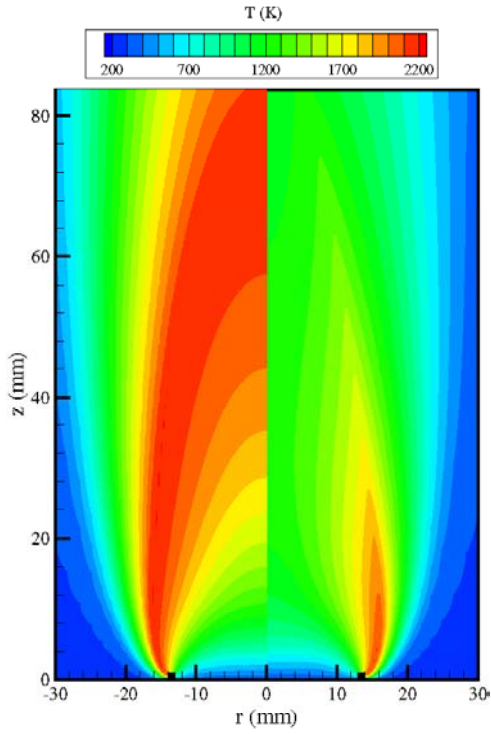


Fig. 4. Zero-g flame calculated using infinitely fast chemistry and without (left) and with (right) radiation.

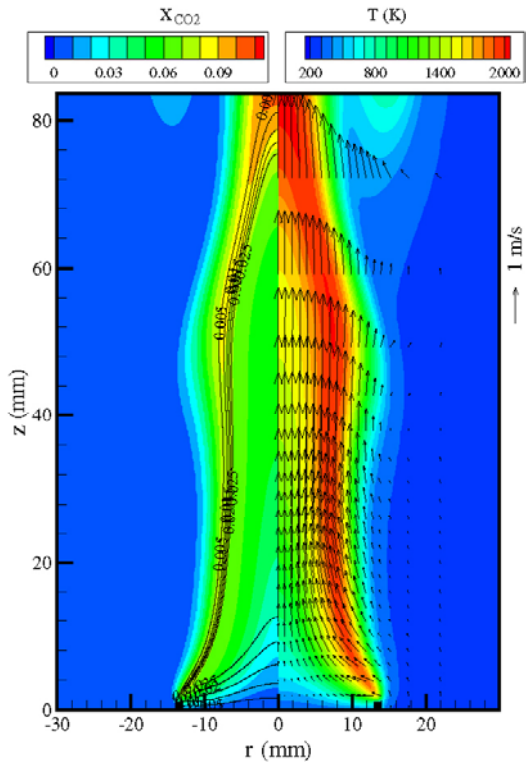


Fig. 5. Normal-gravity flame calculated after ignoring radiative heat losses.

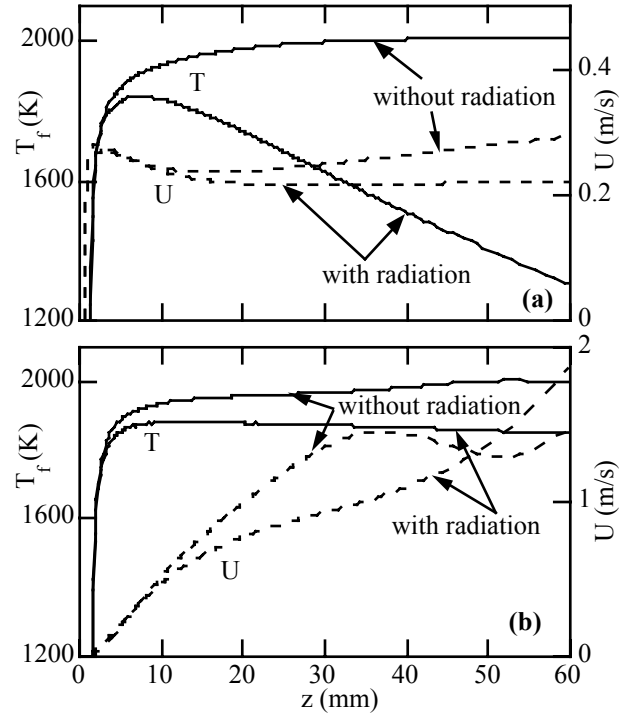


Fig. 6. Variations of temperature and axial velocity with height along the flame surface under (a) normal-gravity and (b) zero-gravity conditions.

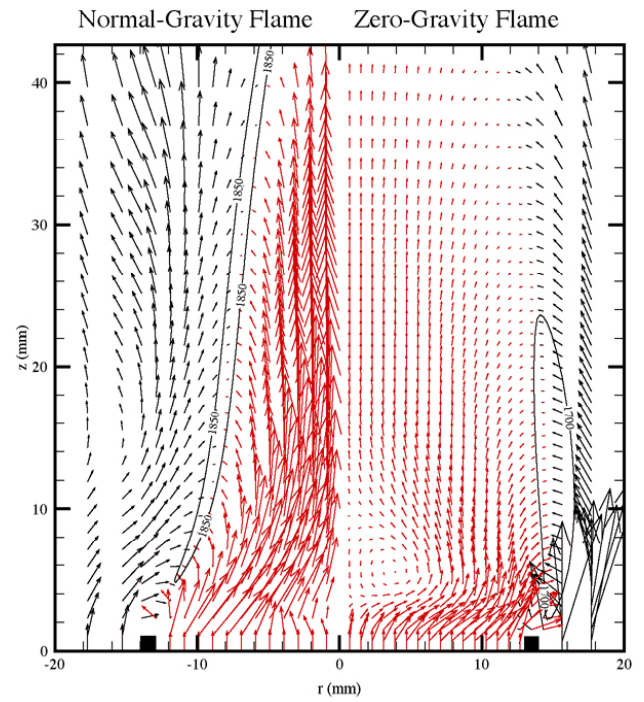


Fig. 7. Fuel and oxidizer fluxes under normal-gravity (left) and zero-gravity (right) conditions.